



APPLICATION OF THE STANDARDIZED VEGETATION INDEX (SVI) AND GOOGLE EARTH ENGINE (GEE) FOR DROUGHT MANAGEMENT IN PERU †

[APLICACIÓN DEL ÍNDICE DE VEGETACIÓN ESTANDARIZADO (SVI) Y GOOGLE EARTH ENGINE (GEE) PARA LA GESTIÓN DE SEQUÍAS EN PERÚ]

Jaris E. Veneros*^{1,2} and Ligia García²

¹Department of Ecology, Montana State University, 1156-1174 S 11th Ave, Bozeman, Montana 59715, USA.

²Instituto de Investigación para el Desarrollo Sustentable de Ceja de Selva (INDES-CES.), Universidad Nacional Toribio Rodríguez de Mendoza de Amazonas. 342 Higos Urco, Chachapoyas 01001, Perú.
Email: jaris.veneros@untrm.edu.pe

*Corresponding author

SUMMARY

Background. The SVI (Standardized Vegetation Index) provides a relative comparison of the condition of the vegetation in different classifications for monitoring droughts. **Objective.** In this research, the SVI was used through the Google Earth Engine (GEE) at the national level and in three study points for a coastal, Amazonian, and Andean region for October 31, 2020, and two decades. **Methodology.** For the construction of the SVI, the data from the Moderate Resolution Imaging Spectroradiometer (MODIS) Version 6 were used; of the Terra sensor (MOD13Q1) with a temporal resolution of 16 days, a spatial resolution of 250 meters, and as a level 3 product. **Results.** The SVI was represented in five classifications: with green color ≥ 0 (No Drought), yellow color -0.10 to -0.94 (Slight drought), light orange color -0.95 to -1.44 (Moderate drought), dark orange color -1.45 to -1.94 (Severe drought), and red color ≤ -1.95 (Extreme drought). **Implications.** The change in historical SVI values was evidenced due to causes such as El Niño costero (coastal) and deforestation of Tropical Forests; for the Sechura Desert in Piura and La Pampa in Madre de Dios, respectively. Subsequently, in the Andes of Peru, in Ollachea, Puno, it was determined that the SVI value, more extreme negative, represented an extreme drought never registered for this area. **Conclusion.** The SVI and GEE provided tools for drought management with high spatial and temporal resolution.

Keywords: SVI; drought; vegetation condition; Google Earth Engine.

RESUMEN

Antecedentes. El SVI (Índice de Vegetación Estandarizado) proporciona una comparación relativa del estado de la vegetación en diferentes clasificaciones para el seguimiento de las sequías. **Objetivo.** En esta investigación se utilizó el SVI a través del Google Earth Engine (GEE) a nivel nacional y en tres puntos de estudio para una región costera, amazónica y andina para el 31 de octubre de 2020 y dos décadas. **Metodología.** Para la construcción del SVI se utilizaron los datos del espectrorradiómetro de imágenes de resolución moderada (MODIS) versión 6; del sensor Terra (MOD13Q1) con una resolución temporal de 16 días, una resolución espacial de 250 metros y como producto de nivel 3. **Resultados.** El SVI se representó en cinco clasificaciones: con color verde ≥ 0 (Sin sequía), color amarillo -0,10 a -0,94 (Sequía leve), color naranja claro -0,95 a -1,44 (Sequía moderada), color naranja oscuro -1,45 a -1,94 (Sequía severa), y color rojo $\leq -1,95$ (Sequía extrema). **Implicaciones.** Se evidenció el cambio en los valores históricos del SVI debido a causas como El Niño costero y la deforestación de los Bosques Tropicales; para el Desierto de Sechura en Piura y La Pampa en Madre de Dios, respectivamente. Posteriormente, en los Andes del Perú, en Ollachea, Puno, se determinó que el valor del SVI, más extremo negativo, representó una sequía extrema nunca registrada para esta zona. **Conclusión.** El SVI y GEE proporcionaron herramientas para la gestión de la sequía con alta resolución espacial y temporal.

Palabras clave: SVI; sequía; estado de la vegetación; Google Earth Engine.

† Submitted May 19, 2021 – Accepted October 25, 2021. This work is licensed under a CC-BY 4.0 International License. ISSN: 1870-0462.

Note: The current version updated the NDVI formula (page 3) on 9/11/2022.

INTRODUCTION

NASA in communication on October 26, 2020, said that there is a severe drought in South America, the first signs of the magnitude of the drought appeared in satellite gravimetry observations of southeastern Brazil since mid-2018 and had spread to parts of Paraguay, Bolivia, and northern Argentina by 2020 (NASA, 2020), considered the second most intense drought in South America since 2002; this alert is based on the extent, duration and volume of water lost during the drought as measured by the GRACE and GRACE-FO satellites (Rodell, 2020). A second announcement alerted the scientific community on November 25, 2020, when the Peruvian National Meteorological and Hydrological Service (SENAMHI) reported that the deficiency of rainfall at the national level will remain of the same magnitude until the following weeks, especially in the central and southern highlands of this country, due to the low humidity in the area (SENAMHI, 2020a). Similarly, rainfall deficiencies at the national level are associated with the entry of dry air from the Pacific, with greater incidence in the southern highlands of Peru (SENAMHI, 2020b; SENAMHI, 2020c), this dry air brought the withdrawal of humidity from the Andes to the east, favoring clear skies and intense radiation during the day and lower temperatures during the night in the central and southern highlands (Fernández, 2020). The humidity forecast for the southern region for November 27 and 28 in 2020 favored the occurrence of localized rainfall in the eastern region and less intensity in the western region, with the possibility of lesser and isolated rains until December of this year (SENAMHI, 2020a). Rainfall deficiencies persisted, especially in the western regions of the Southern Andes. The agricultural sector is affected by increased water stress in Andean dryland crops, as well as by the delay in planting for November in the central and southern highlands of Peru (Fernández, 2020). The impacts caused by SARS-CoV-2 on the agricultural sector, affecting the agri-food chain, added to this problem (García *et al.*, 2020).

The Presidency of the Council of Ministers of Peru on December 1, 2020, issued Supreme Decree No. 149-2020-PCM declaring the State of Emergency for 60 calendar days in 38 provinces and 181 districts of the regions of Tumbes, Piura, Lambayeque, La Libertad, Cajamarca, and Ancash, due to imminent danger of water deficit in the northern part of Peru (SENAMHI, 2020a), this meant the transfer of functions to the regional governments in the implementation of the actions after technical studies, without specifying budget amounts (PCM, 2020).

Otherwise, understanding the relationship between vegetation vigor and moisture availability is complex and has not been adequately studied with satellite sensor data (Ji and Peters, 2003). Drought is a prolonged absence of rainfall, which generates water scarcity over a sufficiently long period so that the lack of precipitation generates a serious hydrological imbalance. Three types of droughts have been determined (Zargar *et al.*, 2011): a. Agricultural drought is the deficit of humidity in the upper meter of the soil, that is, in the root zone, which affects the crops (Skakun *et al.*, 2016). b. Meteorological drought, which is due to prolonged precipitation deficit (Spinoni *et al.*, 2019), and c. Hydrological drought, which is related to below-normal groundwater, lake, and streamflow levels (Shamshirband *et al.*, 2020). Drought studies should consider the duration, magnitude, intensity, severity, geographic extent, and frequency of droughts (Zargar *et al.*, 2011): a. Duration, depending on the region, the duration of drought can vary from one week to a few years. Due to the dynamic nature of drought, a region may experience episodes of drought and rainfall simultaneously when considering various time scales (Kibret *et al.*, 2020). b. Magnitude, the cumulative water deficit; e.g., precipitation, soil moisture, or runoff below a certain threshold during a period of drought (Zargar *et al.*, 2011). c. Intensity, the relationship between the magnitude of the drought and its duration (Kibret *et al.*, 2020). d. Severity, two uses are provided for drought severity; the magnitude of the precipitation deficit, i.e., the magnitude and degree of impacts resulting from the deficit (Xiangtao *et al.*, 2020). e. Geographic extent, the area coverage of the drought that is variable during the event (Ghazaryan *et al.*, 2020); this area can cover several kilometers (Skakun *et al.*, 2016) and f. Frequency or return period, defined as the average time between drought events having a severity equal to or greater than a threshold (Zargar *et al.*, 2011).

Drought monitoring relies on data from geostationary and polar-orbiting satellites, as well as information *in situ* (Chuvienco, 2008). Besides, satellite information can be complemented with studies related to groundwater levels to replenish lakes and reservoirs (Kibret *et al.*, 2020). For example, more than 74 drought indices are known (Zargar *et al.*, 2011), most of them derived from SPI (Standardized Precipitation Indices) and NDVI (Normalized Difference Vegetation Index) (Wainwright *et al.*, 2020). There are also index depending on the purpose of the study; for example, detection and monitoring of droughts in real-time (Ghazaryan *et al.*, 2020), declaration of the beginning or the end of a drought period

(Tarnavsky and Bonifacio, 2020), a study of drought levels and drought response measures (Zargar *et al.*, 2011), analysis of quantitative impacts of droughts on variables at geographic and temporal scales (Tarnavsky and Bonifacio, 2020), finally the declaration of drought conditions among researchers, technicians, organizations and the general public (Adedeji *et al.*, 2020; Tsakiris and Vangelis, 2004; Zargar *et al.*, 2011). These indices currently assist in a variety of operations, such as drought warning, monitoring, and contingency planning.

The reports of Peru's National Center for the Estimation, Prevention and Reduction of Disaster Risk (CENEPRED) based on scientific information from the National Hydrology and Meteorology Service (SENAMHI) and the Multisectoral Committee in charge of the National Study of El Niño costero (ENFEN) regarding droughts or hostile events, are prepared on a regional, provincial or basin scale; however, this information is provided long after the event and therefore hinders the response of decision makers in the process of estimating, preventing and reducing disaster risk (CENEPRED, 2020).

Moderate Resolution Imaging Spectroradiometer (MODIS) Version 6; Terra sensor (MOD13Q1) data are generated every 16 days at a spatial resolution of 250 meters as a level 3 product (Ezzine *et al.*, 2014; Didan, 2020), and are available free of charge at Google Earth Engine (GEE) (Da Silva *et al.*, 2020). The SVI (Standardized Vegetation Index) is based on the calculation of Z-scores, a deviation from the mean NDVI in standardized deviation units at the level of each pixel over a time series (Peters *et al.*, 2002). The SVI allows the time series to be extended with data from the National Oceanic and Atmospheric Administration Advanced Very High-Resolution Radiometer (NOAA-AVHRR) as long as a full inter-calibration between the two sensor systems is provided (Swain *et al.*, 2011). The SVI provides a relative comparison of vegetation conditions, whereas the assessed deviation from the mean vegetation condition cannot be translated into an absolute deviation of plant height, for example. Nor can the SVI be interpreted as an absolute quantification of agricultural damage (Ezzine *et al.*, 2014; Ji and Peters, 2003; Swain *et al.*, 2011).

Understanding the temporal and spatial behavior of precipitation is of high interest, especially in climate risk studies, where the availability of high resolution and good quality information is essential (Carbajal *et al.*, 2010). However, conventional rain gauge measurements are relatively scarce and poorly distributed, especially in developing countries (Asurza and

Lavado, 2018), in this sense., the launch of GEE, a cloud computing platform for storing and processing geographic datasets from local to planetary geographic scale (Gorelick *et al.*, 2017; Kibret *et al.*, 2020), helps in long-term drought monitoring because of the tools it provides (Wang *et al.*, 2012), and for being an important component in early warning systems. Therefore, the objective of this research was to analyze droughts using the Standardized Vegetation Index (SVI) and the GEE for two decades (2000 - 2020) in Peru and to expose their potential for planning and response to drought impacts at local and national scales with a time scale of 16 days.

METHODOLOGY

Standardized Vegetation Index (SVI)

The SVI is used for drought monitoring and early warning of droughts. This index describes the probability of variation of the normal NDVI over several years of data, in a weekly time interval (Peters *et al.*, 2002). SVI is a z-score deviation from the mean in units of standard deviation, calculated from the NDVI (Normalized Difference Vegetation Index) and EVI (Enhanced Vegetation Index) values for each pixel location of a composite period for each year during a given reference period. The SVI formula is shown below (UN-SPIDER, 2020):

$$Z_{ijk} = \frac{VI_{ijk} - \mu_{ij}}{\sigma_{ij}}$$

Where: Z_{ijk} is the z-value for pixel i during week j for year k , VI_{ij} is the weekly VI (Vegetation Index) value for pixel i during week j for year k , so both NDVI and EVI (Son *et al.*, 2014) can be used as VI, μ_{ij} is the mean for pixel i during week j for n years, and σ_{ij} is the standardized deviation of pixel i during week j for n years. This formula was established to obtain data every week; however, due to the temporal resolution of the satellite used in this study, measurements are being taken every 16 days.

For the NDVI and EVI calculations (Son *et al.*, 2014):

$$\text{NDVI} = (P_{nir} - P_{red}) / (P_{nir} + P_{red})$$

$$\text{EVI} = (2.5 * P_{nir} - P_{red}) / (P_{nir} + 6 * P_{red} - 7.5 * P_{blue} + 1)$$

Where: P_{red} : (620–670 nm), P_{nir} (841–876 nm), and P_{blue} (459–479 nm) are MODIS bands 1, 2, and 3

The SVI calculation is based on the EVI, which in turn is obtained from the corrected NDVI, has improved sensitivity in dense vegetation conditions, and is less affected by the influence of aerosols (Wang *et al.*, 2012). The random variable of a standardized normal distribution corresponds to a Z-score. Therefore; each random variable X can be transformed into a Z-score by the following equation (UN-SPIDER, 2020):

$$Z = (X - \mu) / \sigma$$






Where X is a normal random variable, μ is the mean and σ is the standard deviation. Therefore, a Z-score equal to 0 represents an element equal to the mean, a Z-score less than 0 represents an element less than the mean, and a Z-score greater than 0 represents an element greater than the mean. The Z-score indicates how many standard deviations an item is from the mean, so the standard deviation, in general, indicates how dispersed the data set is (Peters *et al.*, 2002). A low standard deviation implies that the data are tightly clustered around the mean, while a high standard deviation implies that the data are spread over a wider range of values. If the number of elements in the data set is large, approximately 68% of the data are within 1 standard deviation from the mean, 95% within 2 standard deviations, and 99.7% within 3 standard deviations from the mean, when it is a normal distribution. The SVI was represented in five categories (Table 1) (UN-SPIDER, 2020): SVI with green color ≥ 0 (No Drought), yellow color -0.10 to -0.94 (Mild Drought), light orange color -0.95 to -1.44 (Moderate Drought), dark orange color -1.45 to -1.94 (Severe Drought) and red color ≤ -1.95 (Extreme Drought). The SVI dynamics can be influenced by rainfall, stress, phenology, flooding, pests and diseases, nutrient deficiencies, forest fires, grazing and human activities (Ji Peters, 2003). However, the factors mentioned above must be associated with the types of droughts as well as the duration, magnitude, intensity, severity, geographic extent, and frequency to understand the droughts (Zargar *et al.*, 2011). Finally, we used the coefficient of variation to determine the statistical measure of the dispersion of the data points around the mean of the calculated SVI and box plots to show the dispersion of the SVI data in the study areas. These box plots are a standardized method of graphically representing a series of SVI numerical data through their quartiles.

SVI Nacional

The Standardized Vegetation Index (SVI) was used for drought analysis at the national level using the method developed by UFSM in Brazil

in cooperation with UN-SPIDER within the SEWS-D project (UN-SPIDER, 2020); MODIS images were used: ee.ImageCollection ("MODIS/006/MOD13Q1") from GEE (Didan *et al.*, 2015), from October 31, 2020.

Table 1. Drought classes according to the value of the Standardized Vegetation Index (SVI) for Peru

Class	Value	Color
Extreme Drought	≤ -1.95	
Severe Drought	-1.45 a -1.94	
Moderate Drought	-0.95 a -1.44	
Mild Drought	-0.10 a -0.94	
No Drought	≥ 0	

Historical SVI

The historical values and trends of SVI recorded in two decades (2000-2020), were obtained with a spatial resolution of 250 m and a temporal resolution of 16 days, applying as examples of cases of one pixel per Region: Coastal (Sechura Desert, Piura), Andean (Ollachea, Puno) and Amazonian (La Pampa, Madre de Dios) zones.

Terra-Modis vegetation indices

The MOD13Q1 V6 product available from GEE provides a Vegetation Index (VI) value per pixel of 250 m, where there are two vegetation layers: the first is the NDVI and the second vegetation layer is the EVI which minimizes canopy background variations and maintains sensitivity in dense vegetation conditions (Didan *et al.*, 2015). EVI also uses the blue band to remove residual air pollution caused by smoke and thin sub-pixel clouds (Ronchetti *et al.*, 2020). MODIS products such as NDVI and EVI are calculated from atmospherically corrected bidirectional surface reflectance that has been masked for water, clouds, heavy aerosols, and cloud shadows (UN-SPIDER, 2020).

Study area

The Republic of Peru is a country located in South America and has a total area of 1 285 215 km². It borders the Pacific Ocean to the west, Ecuador and Colombia to the north, Brazil to the east, Bolivia to the southeast, and Chile to the south. For this research, we used the shapefiles of Peru at the Adm0 and Adm1 levels of the GADM Portal version 2.8 (GADM, 2018). The Andes Mountain Range determines different geomorphologic units of a continental and marine environment for Peru (González-Moradas Viveen, 2020). From west to east, in the continental area, the units correspond to 1.

Coastal Cordillera; 2. Pre-Andean Plain; 3. Western Cordillera; 4. Inter-Andean Depressions; 5. Eastern Cordillera; 6. Titicaca Basin; 7. Sub-Andean Region; and 8. Amazonian Plain and in the marine field, the units include 1. Continental Shelf; 2. Continental Slope; 3. Marine Trench; 4. Nazca Ridge; and 5. South Pacific Abyssal Sea Floor (INGEMMET, 1995).

Concerning the climate, Peru has eight natural regions (Pulgar, 2014): Chala or coast, yunga, quechua, suni, puna, janca or mountain range, high jungle, and low jungle. Therefore, Peru has a diversity of climates and microclimates from the arid and warm coastal, through the inter-Andean valleys of temperate, frigid, and polar type to the warm and rainy type of the jungle (SENAMHI, 2020b). Three factors determine Peru's climate: the country's location in the intertropical zone, the altitudinal changes

introduced by the Andes Mountains, and the flow along the country's coasts (INGEMMET, 1995).

Sechura Desert, Piura - Coast Region

A random point of geographic coordinates was selected -5.315960, -81.034303 using the ArcGis ver. 10.7 tool called Arc Toolbox: Data Management Tools > Feature Class > Create Random Points (Figures 1A, 2A y 3A). It is located in the Sechura Desert, in the Piura Region, with an average altitude of 11 masl, an average annual maximum temperature of 30 °C, an average annual minimum temperature of 23 °C and an average annual rainfall of 16 mm (SENAMHI, 2020b). This point presents an ecosystem of the coastal desert type, i.e., arid to hyper-arid climate with areas mostly devoid of vegetation consisting of sandy soils or rocky outcrops in flat, undulating, and dissected areas subject to wind erosion (MINAM, 2018).

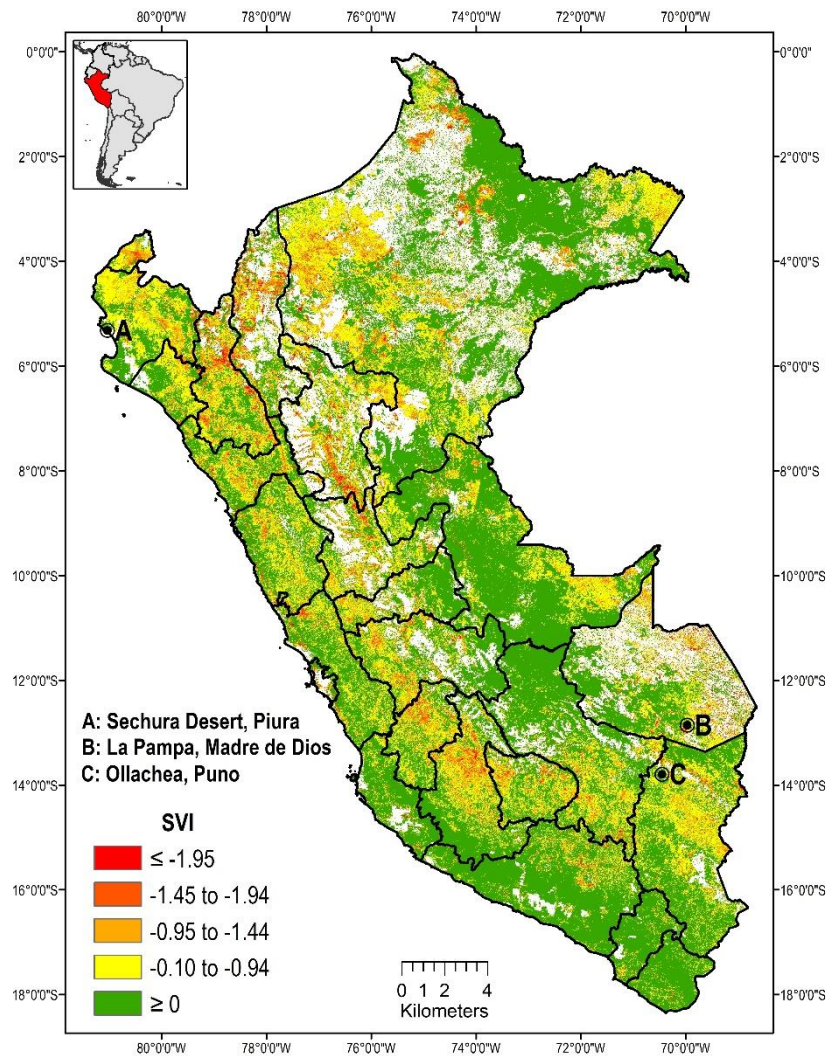


Figure 1. Standardized Vegetation Index (SVI) in Peru.

La Pampa, Madre de Dios - Jungle Region

In the Madre de Dios Region, a random point was established with the following geographic coordinates -12.853405, -69.972633 (Figures 1B, 2B, and 3B), this point belongs to the place called La Pampa. It has an average altitude of 203 masl, an average maximum temperature of 31 °C, an average minimum temperature of 20 °C and shows average annual precipitation of 2221 mm (Figures 1B, 2B and 3B) (SENAMHI, 2020b). This point is within an area dedicated to illegal mining and belongs to a buffer zone of the Tambopata National Reserve. The ecosystem is an alluvial landscape in the Amazonian plain, which is periodically flooded by normal floods of 5 to 8 meters in height. The forest with sparse or open undergrowth can have 3 or 4 strata with a canopy or dome of trees that reach 20 to 25 meters high and emergent individuals up to 30 meters high (MINAM, 2018).

Ollachea, Puno - Andes Region

In the Puno Region, a random point was selected with the geographic coordinates -13.792852, -70.453065 (Figures 1C, 2C, and 3C), which belongs to the Ollachea District. It has an average altitude of 2659 masl, an average maximum temperature of 22 °C, an average minimum temperature of 7 °C, and average annual precipitation of 1360 mm (Figures 1C, 2C, and 3C) (SENAMHI, 2020b). This point presents an ecosystem of the Pajonal type of humid puna (MINAM, 2018).

RESULTS AND DISCUSSIONS

Regional Standardized Vegetation Index (SVI)

It was determined that, as of October 31, 2020, SVI values in all regions of Peru presented ranges from extreme drought values (≤ -1.95 ; red color) to non-drought values (≥ 0 ; green color) (Table 1, Figure 1).

SVI dynamics can be influenced by precipitation, stress, phenology, flooding, pests and diseases, nutrient deficiency, forest fires, grazing, and human activities (Ji Peters, 2003). The coefficients of variation of the SVI range from 124.08% in Arequipa to 1691.75% in Puno (Table 2, Figure 1); a situation that merits that the analysis of the drought indexes should be performed independently for each region, as well as the meteorological conditions, especially if the seasons of the year are marked, such as autumn and winter (Table 2, Figure 1) (Ezzine *et al.*, 2014), because the most common statistical methods applied to NDVI and precipitation time series, such as simple linear correlation or regression analyses, produce inaccurate results if seasonality is not taken into account (Ji Peters, 2003).

The values for extreme droughts (minimum SVI, ≤ -1.95) exceed up to 2.16 times the classification limit value (UN-SPIDER, 2020), as in the case of the Ayacucho Region (-4.23), or 1.57 times as in the case of the Tumbes Region (-3.08) (Table 2; Figure 1); this showed that these places deserve special attention due to their low water availability. Recalling that, in addition to this

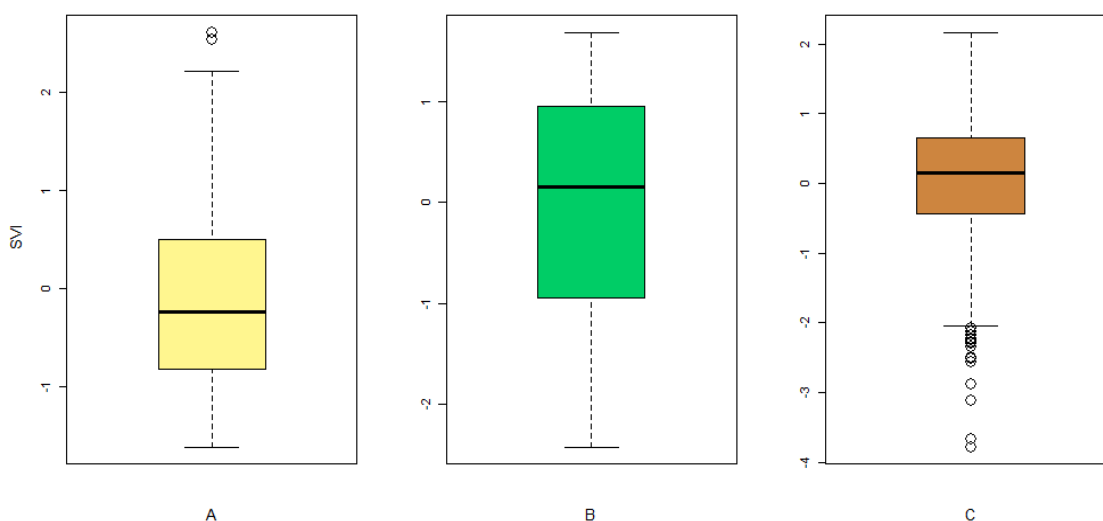


Figure 2. Historical values for the Standardized Vegetation Index (SVI) for three pixels every 16 days from February 18, 2000 to October 31, 2020. Where: **A.** Sechura Desert, Piura **B.** La Pampa, Madre de Dios, and **C.** Ollachea, Puno.

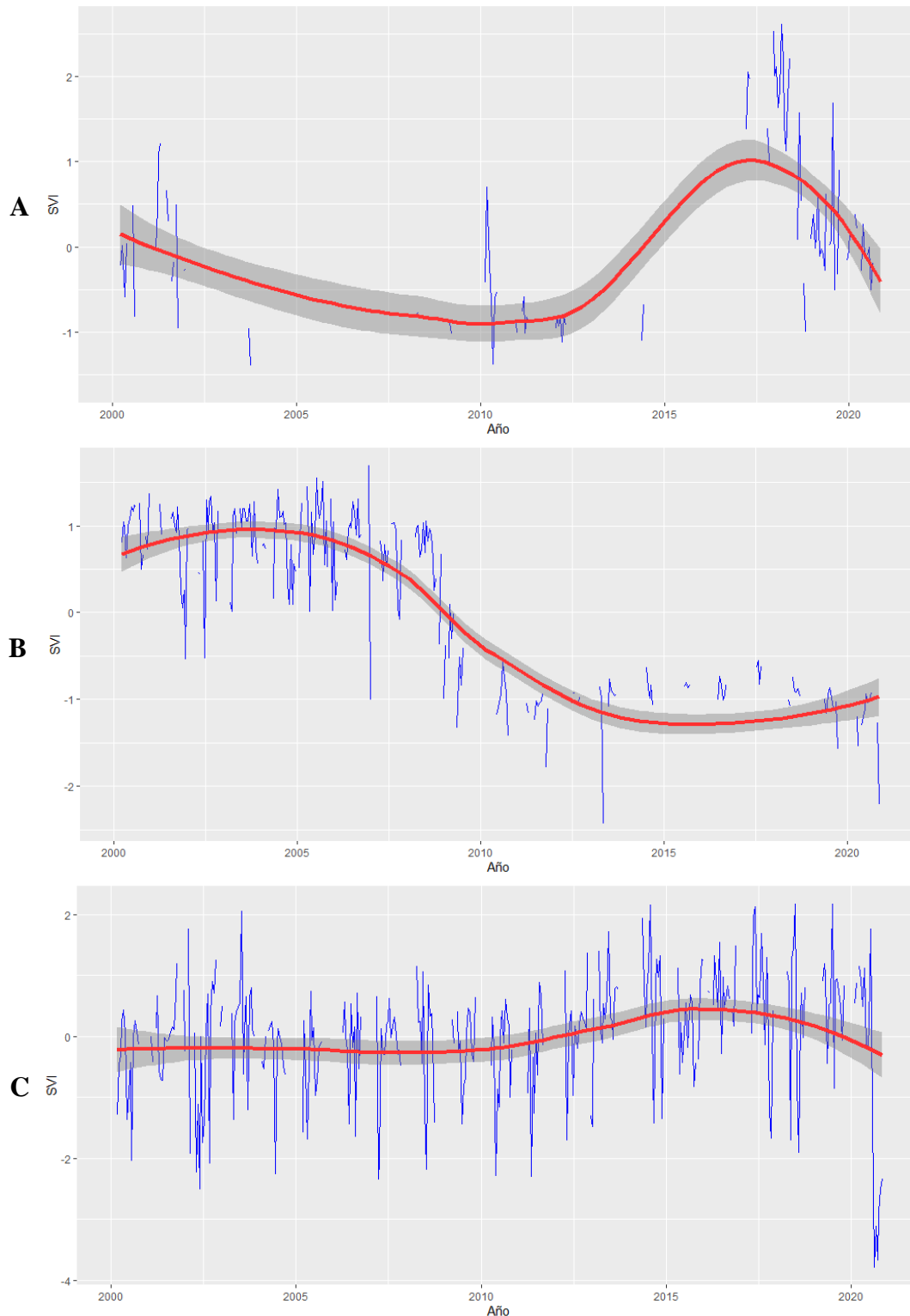


Figure 3. Trends of historical values for the Standardized Vegetation Index (SVI) from February 18, 2000 to October 31, 2020. Where: **A.** Sechura Desert, Piura **B.** La Pampa, Madre de Dios, and **C.** Ollachea, Puno.

problem, there are the impacts caused by SARS-CoV-2 on the Peruvian agricultural sector, in terms of quantity and the need to distribute food for food security (García *et al.*, 2020).

In Peru, SENAMHI uses interpolated climatological and hydrological data with a resolution of 5 km to study rainfall and droughts (Risco Sence *et al.*, 2017), but drought analysis based on Terra Modis data identifies patterns of drought-prone areas (Uttaruk Laosuwan, 2019)

at a resolution of 250 m (Didan, 2020), which provides more timely data for technical studies on drought management, as requested by the central government in its decree on drought management N° 149-2020-PCM (PCM, 2020). Adjusting the SVI data obtained from satellites with SENAMHI observations may be of potential use for drought studies, depending on the availability of data from the national network of meteorological stations in Peru.

Sechura Desert, Piura Region

The study point with geographical coordinates -5.315960, -81.034303 (Figure 1A), in the Sechura Desert, Piura Region, presented a minimum SVI of -3.34 corresponding to extreme drought (Table 1); with a coefficient of variation of 360.67 % in the two decades (Table 2). This point is in the Sechura Desert, a pixel with mostly negative values due to the natural conditions of its ecosystem. Figures 2A and 3A, show that in April 2017 there was an increase of SVI up to 3.5 (No drought), the atypical value within the two decades and represented by the appearance of vegetation conditions according to the SVI interpretation. This is consistent with the rains that occurred on those dates when it was declared an area impacted by El Niño costero (coastal) (Salazar *et al.*, 2019). These precipitations generated the greening of some parts of the Sechura Desert, according to NASA Worldview satellite views. Finally, the most intense rains in Piura occurred on March 26, with a duration of 15 hours of rain, so that on March 27, the Piura River overflowed its banks with a flow of 3,016 m³/s, flooding Piura, Castilla, and agricultural areas (Salazar *et al.*, 2019; Villa Aurelien, 2020).

La Pampa, Madre de Dios Region

Droughts should be evaluated not only by the presence or absence of rainfall but also by surrounding factors that allow identifying, for example, regeneration patterns after fires (Chuvieco *et al.*, 2020), adding studies of geographic variables such as topography, soil characteristics, or climate or relevance of burn severity. For example, in La Pampa, Madre de Dios Region, for the study point with geographic coordinates -12.853405, -69.972633 (Figure 1B), historical values were identified for the two decades of SVI with extreme droughts (maximum SVI: -3.62) (Figures 2B and 3B), corroborating the loss of tropical forests to bare soils, where illegal mining activities have been deforesting since before 1999 (Figures 2B and 3B) (Asner Tupayachi, 2017). The negative values of this SVI corroborate the lack of vegetation conditions for this zone, so it is suggested that this index complements the

management of deforestation monitoring. Therefore; negative values in the SVI may be due to deforestation and the presence of bare soil.

Ollachea, Puno Region

At the point under study, with geographical coordinates, -13.792852, -70.453065 (Figure 1C), Ollachea district, Puno Region, presented a minimum SVI for the two decades of -3.97 (extreme drought) (Table 1) with a coefficient of variation 1691.75 % (Table 2). The SVI presents extreme negative outliers for 2020 (Figures 2C and 3C); the most extreme value -3.97; was recorded for August 12, 2020, followed by other extreme values observed in August and September, -3.10 and -3.66 respectively, all these values correspond to Extreme Drought (Table 1). According to a SENAMHI report, the Puno Region had a 95% rainfall deficit for November, and since October 24, 2020, rainfall was insignificant in most of the stations of the Puno highlands (SENAMHI, 2020d).

Drought management should be done at a high spatial scale and high geographic extent, identifying water sources, water balances and examining downstream river flows (Gutiérrez *et al.*, 2005; Phillips *et al.*, 2009), droughts are more recurrent due to the lack of focus on the protection of water sources (Garcia and Otto, 2015). Countries such as Brazil used the ESG to support restoration policy measures within environmental sciences, territorial planning, and subsidy for the enforcement of environmental law (C. Silva Junior *et al.*, 2020). In this sense, it has been identified that the origins of the Amazon River area in the Peruvian Andes (Anderson *et al.*, 2018), and drought management in emergencies should be declared at the source, not only downstream, as has happened with rivers in the Pacific, Atlantic or Titicaca basins (Lavado-Casimiro and Espinoza, 2014).

The actions taken by the Peruvian Government in the face of drought emergencies are oriented solely to the purchase of products, for example, water supplies for livestock, foliar fertilizers, supplementary feed, among others in the Cajamarca Region (COEN, 2020), comprehensive drought mitigation strategies are urgently needed.

Finally, the SVI was obtained from a deviation of the z-score (pixel) from the mean in standard deviation units, calculated from NDVI and EVI values (Peters *et al.*, 2002) in the Google Earth Engine (GEE), at the national level and historical trends in Peru for two decades. The SVI presented advantages concerning meteorological

Table 2. Values for the Standardized Vegetation Index (SVI) for October 31, 2020 in the Regions of Peru

Region	N	SVI _{minimum}	SVI _{maximum}	SVI _{average}	SD _{SVI}	CV _{SVI} %
Amazonas	78610	-3.62	3.50	-0.39	1.10	281.49
Ancash	107349	-3.81	4.28	-0.07	0.83	1139.23
Apurímac	64760	-3.62	3.82	-0.18	0.88	489.96
Arequipa	198522	-4.07	4.37	0.94	1.16	124.08
Ayacucho	116550	-4.23	4.36	0.10	1.12	1107.22
Cajamarca	100991	-3.61	3.14	-0.44	0.90	205.35
Cusco	195687	-3.92	3.94	0.24	0.82	345.78
Huancavelica	60244	-3.34	3.77	-0.21	0.85	402.04
Huánuco	94126	-3.18	3.70	-0.20	0.89	440.11
Ica	55308	-4.18	4.47	0.82	1.11	135.18
Junín	124599	-3.23	3.33	0.07	0.95	1291.16
La Libertad	85503	-3.47	4.45	-0.08	0.92	1104.44
Lambayeque	46092	-3.43	4.36	-0.09	0.85	969.85
Lima y Callao	102750	-3.78	4.32	0.14	0.93	655.13
Loreto	955497	-3.62	3.69	0.14	0.94	661.04
Madre de Dios	170387	-3.37	2.85	-0.12	0.98	802.63
Moquegua	41178	-4.11	4.31	1.19	1.16	96.82
Pasco	70765	-3.22	3.18	0.19	0.93	488.83
Piura	119186	-3.34	4.12	-0.22	0.78	360.67
Puno	184763	-3.97	4.04	0.05	0.86	1691.75
San Martín	104387	-3.71	3.43	-0.41	0.92	226.61
Tacna	46115	-4.01	4.34	1.09	1.09	99.39
Tumbes	15791	-3.08	2.69	-0.69	0.73	105.82
Ucayali	350644	-3.74	3.44	0.35	0.75	215.42

N=Number of pixels per Region; SVI_{minimum}=Lowest SVI value by region; SVI_{maximum}= Highest SVI value by region; SVI_{average}=Average SVI value by region; SD_{SVI}= Standard deviation for the SVI by region and CV_{SVI} %= Coefficient of variation of SVI by region.

drought indices (Ji and Peters, 2003). It was possible to work with a high spatial resolution at the national level (250 m) and to cover larger areas (Gorelick *et al.*, 2017). A temporal resolution of 16 days allows better management to face droughts in Peru; achieving values for the severity of vegetation stress resulting from a water deficit (Wang *et al.*, 2012) or other phenomena that cause the loss of water content in plants.

CONCLUSIONS

The Standardized Vegetation Index (SVI) was determined for a specific date throughout Peru, as well as for two decades in three study points using the GEE. The change of the SVI values due to causes such as El Niño Phenomenon for the Sechura Desert, Piura, and deforestation in Tropical Forests in the La Pampa Zone, Madre de Dios, was verified. Subsequently, in the Peruvian Andes, in Ollachea, Puno, it was determined that the most extreme negative SVI value represented an extreme drought never recorded for this area. Finally, the GEE provided free of charge a

historical series of satellite images from 2000 to date, at the local and national level with a spatial scale of 250 m and a temporal scale of 16 days for drought studies for Peru.

Acknowledgments

Thanks to the Instituto de Investigación para el Desarrollo Sustentable de Ceja de Selva (INDES-CES) of the Universidad Nacional Toribio Rodríguez de Mendoza of Amazonas (Peru) and Montana State University (USA) for the academic support.

Funding. This project was financed by the Instituto de Investigación para el Desarrollo Sustentable de Ceja de Selva (INDES-CES) de la Universidad Nacional Toribio Rodríguez de Mendoza de Amazonas (Perú) mediante el Proyecto del Sistema Nacional de Inversión Pública (SNIP) N° 352431 “Creación de los Servicios del Centro de Investigación en Climatología y Energías Alternativas” (PROCICEA) y la Universidad Estatal de Montana (Estados Unidos).

Conflict of interests. The authors declare that there is no conflict of interest related to this publication.

Compliance with ethical standards. Nothing to declare/does not apply.

Data availability. Data is available from the corresponding author upon request.

Author contribution statement.

Jaris E. Veneros – Conceptualization, Data curation, Formal Analysis, Investigation, Methodology, Software, Supervision, Validation, Visualization, Writing – original draft, Writing – review and editing., **Ligia García** – Project administration, Formal Analysis, Investigation, Methodology, Resources, Writing – original draft, Writing – review and editing.

REFERENCES

- Adedeji, O., Olusola, A., James, G., Shaba, H. A., Orimoloye, I. R., Singh, S. K., and Adelabu, S., 2020. Early warning systems development for agricultural drought assessment in Nigeria. *Environmental Monitoring and Assessment*, 192(12), pp. 1–21. <https://doi.org/10.1007/s10661-020-08730-3>
- Anderson, E. P., Jenkins, C. N., Heilpern, S., Maldonado-Ocampo, J. A., Carvajal-Vallejos, F. M., Encalada, A. C., Rivadeneira, J. F., Hidalgo, M., Cañas, C. M., Ortega, H., Salcedo, N., Maldonado, M., and Tedesco, P. A., 2018. Desierto de Sechura - Piura. *Science Advances*, 4(1), pp. 1–8. <https://doi.org/10.1126/sciadv.aao1642>
- Andina Agencia Peruana de Noticias, 2020. Comunidad de Ollachea tendrá participación de 5% en proyecto aurífero, señala Minera IRL. En *Andina*. Último Acceso: 25 de diciembre, 2020 de <https://andina.pe/agencia/noticia-comunidad-ollachea-tendra-participacion-5-proyecto-aurifero-senala-minera-irl-370149.aspx>
- Asurza, F., Ramos, C., and Lavado, W., 2018. Evaluación de los productos Tropical Rainfall Measuring Mission (TRMM) y Global Precipitation Measurement (GPM) en el modelamiento hidrológico de la cuenca del río Huancané, Perú. *Scientia Agropecuaria*, 9(1), pp. 53-62. <https://doi.org/10.17268/sci.agropecu.2018.01.06>
- Carbajal, C. M., Yarlequé, C., and Posadas, A., 2010. Datos faltantes de precipitación pluvial diaria mediante la Transformada Wavelet. *Revista Peruana Geo-Atmosférica*, 88(2), pp. 76-88. <https://repositorio.senamhi.gob.pe/bitstream/handle/20.500.12542/1069/Reconstrucci%C3%B3n-de-datos-faltantes-de-precipitaci%C3%B3n-pluvial-diaria-mediante-la-Transformada-Wavelet.pdf?sequence=1&isAllowed=y>
- CENEPRED, 2020. Temporada de lluvia 2020 – 2021: escenario de riesgo por déficit de lluvias en la costa y sierra norte del Perú para el periodo setiembre – noviembre 2020. pp. 1–22. En *CENEPRED*. Último acceso: 20 de diciembre, 2020 de https://cenepred.gob.pe/web/wp-content/uploads/2020/09/ESCENARIO-DE-RIESGO-DEFICIT_PP.pdf
- Chuvieco, E., 2008. Earth observation of global change: the role of satellite remote sensing in monitoring the global environment. In *Earth Observation of Global Change: The Role of Satellite Remote Sensing in Monitoring the Global Environment*. Alcalá de Henares: Springer.
- COEN, 2020. Reporte de peligro inminente N° 148 - 21/12/2020 / COEN - INDECI / 17:45 HORAS (Reporte N° 3) por déficit hídrico en el departamento de Cajamarca. En *INDECI*. Último acceso: 20 de diciembre, 2020 de <https://www.indeci.gob.pe/wp-content/uploads/2020/12/REPORTE-DE-PELIGRO-INMINENTE-N%C2%BA-148-21DIC2020-PELIGRO-POR-DEFICIT-HIDRICO-EN-EL-DEPARTAMENTO-DE-CAJAMARCA-3.pdf>
- Da Silva, C. A., Leonel-Junior, A. H. S., Rossi, F. S., Correia Filho, W. L. F., Santiago, D. de B., de Oliveira-Júnior, J. F., Teodoro, P. E., Lima, M., and Capristo-Silva, G. F., 2020. Mapping soybean planting area in midwest Brazil with remotely sensed images and phenology-based algorithm using the Google Earth Engine platform. *Computers and Electronics in Agriculture*, 169(2019), pp. 1–10. <https://doi.org/10.1016/j.compag.2019.105194>
- Didan, K., 2020. LP DAAC - MOD13Q1 MODIS/Terra vegetation indices 16-

- Day L3 global 250 m SIN Grid. En *USGS*. Último acceso: 20 de diciembre, 2020 de <https://lpdaac.usgs.gov/products/mod13q1v006/>
- Didan, K., Munoz, A. B., Solano, R., and Huete, A., 2020. MODIS vegetation index user's guide (Collection 6). En *Modis Active Fire and Burned Area Products*. Último acceso: 20 de diciembre, 2020 de https://modis-fire.umd.edu/files/MODIS_C6_Fire_User_Guide_C.pdf
- Ezzine, H., Bouziane, A., and Ouazar, D., 2014. Seasonal comparisons of meteorological and agricultural drought indices in Morocco using open short time-series data. *International Journal of Applied Earth Observation and Geoinformation*, 26(1), 36–48. <https://doi.org/10.1016/j.jag.2013.05.005>
- Fernández, C., 2020. Puno: ausencia de lluvias en el altiplano preocupa a los agricultores. En *El Comercio*. Último acceso: 21 de diciembre, 2020 de <https://elcomercio.pe/peru/puno/puno-ausencia-de-lluvias-en-el-altiplano-preocupa-a-los-agricultores-noticia/>
- GADM, 2020. Database of global administrative areas version 2.8 (GADM). En *GADM maps and data*. Último acceso: 21 de diciembre, 2020 de <https://gadm.org/>
- García, E., and Otto, M., 2015. Caracterización ecohidrológica de humedales alto andinos usando imágenes de satélite multitemporales en la cabecera de cuenca del Río Santa, Ancash, Perú. *Ecología Aplicada*, 14(2), 2015. <http://www.scielo.org.pe/pdf/ecol/v14n2/a04v14n2.pdf>
- García, L., Veneros, J., and Tineo, D., 2020. Severe acute respiratory syndrome (SARS-CoV-2): A national public health emergency and its impact on food security in Peru. *Scientia Agropecuaria*, 11(2), pp. 241–245. <https://doi.org/10.17268/SCI.AGROPE.CU.2020.02.12>
- Ghazaryan, G., Dubovyk, O., Graw, V., Kussul, N., and Schellberg, J., 2020. Local-scale agricultural drought monitoring with satellite-based multi-sensor time-series. *GIScience and Remote Sensing*, 57(5), pp. 704–718. <https://doi.org/10.1080/15481603.2020.1778332>
- GMC, 2020. Desierto de Sechura - Piura. En *Pinterest*. Último acceso: 01 de diciembre, 2020 de <https://www.pinterest.com/pin/569846159084164271/>
- González-Moradas, M. del R., and Viveen, W., 2020. Evaluation of ASTER GDEM2, SRTMv3.0, ALOS AW3D30 and TanDEM-X DEMs for the Peruvian Andes against highly accurate GNSS ground control points and geomorphological-hydrological metrics. *Remote Sensing of Environment*, 237(2020), pp. 1-19. <https://doi.org/10.1016/j.rse.2019.111509>
- Gorelick, N., Hancher, M., Dixon, M., Ilyushchenko, S., Thau, D., and Moore, R., 2017. Google earth engine: planetary-scale geospatial analysis for everyone. *Remote Sensing of Environment*, 202, pp. 18–27. <https://doi.org/10.1016/j.rse.2017.06.031>
- Gutiérrez, C., Ochoa, L., and Velasco, I., 2005. Sequía, un problema de perspectiva y gestión. *Región y Sociedad*, 17(34), pp. 35–71. <http://www.scielo.org.mx/pdf/regsoc/v17n34/v17n34a2.pdf>
- INGEMMET, 2020. Geología del Perú. En *Instituto Geológico, Minero y Metalúrgico - INGEMMET*. Último acceso: 01 de diciembre, 2020 de <https://repositorio.ingemmet.gob.pe/handle/20.500.12544/176>
- Isminas Revista, 2020. La desgracia de vivir en la riqueza. En *La Oreja Roja*. Último acceso: 01 de diciembre, 2020 de <https://www.laorejaroja.com/la-desgracia-de-vivir-en-la-riqueza/>
- Ji, L., and Peters, A. J., 2003. Assessing vegetation response to drought in the northern Great Plains using vegetation and drought indices. *Remote Sensing of Environment*, 87(1), pp. 85–98. [https://doi.org/10.1016/S0034-4257\(03\)00174-3](https://doi.org/10.1016/S0034-4257(03)00174-3)
- Kibret, K. S., Marohn, C., and Cadisch, G., 2020. Use of MODIS EVI to map crop phenology, identify cropping systems, detect land use change and drought risk in Ethiopia—an application of Google Earth Engine. *European Journal of Remote Sensing*, 53(1), pp. 176–191. <https://doi.org/10.1080/22797254.2020.1786466>
- Lavado-Casimiro, W., and Espinoza, J. C., 2014. Impactos de el niño y la niña en las lluvias del Perú (1965-2007). *Revista*

- Brasileira de Meteorologia*, 29(2), pp. 171–182.
<https://doi.org/10.1590/S0102-77862014000200003>
- MINAM, 2020. Mapa nacional de ecosistemas del Perú. En *SINIA-Sistema Nacional de Información Ambiental*. Último acceso: 01 de diciembre, 2020 de <https://sinia.minam.gob.pe/mapas/mapa-nacional-ecosistemas-peru>
- NASA, 2020. Severe drought in South America. En *Earth Observatory*. Último acceso: 01 de diciembre, 2020 de <https://earthobservatory.nasa.gov/images/147480/severe-drought-in-south-america>
- PCM, 2020. Decreto Supremo que declara el Estado de Emergencia en varios distritos de algunas provincias de los departamentos de Tumbes, Piura, Lambayeque, La Libertad y Cajamarca, por peligro inminente ante déficit hídrico. En *El Peruano*. Último acceso: 15 de diciembre, 2020 de <https://busquedas.elperuano.pe/normaslegales/decreto-supremo-que-declara-el-estado-de-emergencia-en-vario-decreto-supremo-n-149-2020-pcm-1884523-1/>
- Peters, A. J., Walter-Shea, E. A., Ji, L., Viña, A., Hayes, M., and Svoboda, M. D., 2002. Drought monitoring with NDVI-based standardized vegetation index. *Photogrammetric Engineering and Remote Sensing*, 68(1), pp. 71–75.
- Phillips, O. L., Aragão, L. E. O. C., Lewis, S. L., Fisher, J. B., Lloyd, J., López-González, G., Malhi, Y., Monteagudo, A., Peacock, J., Quesada, C. A., Van Der Heijden, G., Almeida, S., Amaral, I., Arroyo, L., Aymard, G., Baker, T. R., Bánki, O., Blanc, L., Bonal, D., and Torres-Lezama, A., 2009. Drought sensitivity of the amazon rainforest. *Science*, 323(5919), 1344–1347. <https://doi.org/10.1126/science.1164033>
- Pulgar, J., 2014. Las ocho regiones naturales del Perú. *Terra Brasilis*, 3, 1–19. <https://doi.org/10.4000/terrabrasilis.1027>
- Risco Sence, E., Casimiro, W. L., and Mejia Marcacuzco, A., 2017. Runoff generation at Sub-Basin scale in Peru (Pacific and Titicaca Basins). En *E-Proceedings of the 38th IAHR World Congress*. Ciudad de Panamá, Panamá., 1–6 Septiembre. pp. 4702–4710
- Rodell, M., 2020. Esta es la segunda sequía más intensa en América del Sur desde 2002. En *La República*. Último acceso: 15 de diciembre, 2020 de <https://larepublica.pe/ciencia/2020/11/09/esta-es-la-segunda-sequia-mas-intensa-en-america-del-sur-desde-2002/>
- SENAMHI, 2020. a. Continuará la ausencia de lluvia en sierra central y sur. En *Plataforma digital única del Estado Peruano*. Último acceso: 13 de diciembre, 2020 de <https://www.gob.pe/institucion/senamhi/noticias/317152-continuara-la-ausencia-de-lluvia-en-sierra-central-y-sur>
- SENAMHI, 2020b. Mapa climático del Perú. En *SENAMHI*. Último acceso: 13 de diciembre, 2020 de <https://www.senamhi.gob.pe/servicios/?p=mapa-climatico-del-peru>
- SENAMHI, 2020c. Reporte climático de lluvias a nivel Nacional: setiembre – noviembre 2020. En *Plataforma digital única del Estado Peruano*. Último acceso: 13 de diciembre, 2020 de <https://www.gob.pe/qu/institucion/senamhi/informes-publicaciones/1412533-reporte-de-climatico-de-lluvias-a-nivel-nacional-setiembre-noviembre-2020>
- Shamshirband, S., Hashemi, S., Salimi, H., Samadianfard, S., Asadi, E., Shadkani, S., Kargar, K., Mosavi, A., Nabipour, N., and Chau, K. W., 2020. Predicting Standardized Streamflow index for hydrological drought using machine learning models. *Engineering Applications of Computational Fluid Mechanics*, 14(1), pp. 339–350. <https://doi.org/10.1080/19942060.2020.1715844>
- Silva, C., Heinrich, V., Freire, A., Broggio, I., Rosan, T., Doblas, J., Anderson, L., Rousseau, G., Shimabukuro, Y., Silva, C., House, J., and Aragão, L., 2020. Benchmark maps of 33 years of secondary forest age for Brazil. *Scientific Data*, 7(1), pp. 1–9. <https://doi.org/10.1038/s41597-020-00600-4>
- Skakun, S., Kussul, N., Shelestov, A., and Kussul, O., 2016. The use of satellite data for agriculture drought risk quantification in Ukraine. *Geomatics, Natural Hazards and Risk*, 7(3), pp. 901–917. <https://doi.org/10.1080/19475705.2015.1016555>
- Son, N. T., Chen, C. F., Chen, C. R., Minh, V.

- Q., and Trung, N. H., 2014. A comparative analysis of multitemporal MODIS EVI and NDVI data for large-scale rice yield estimation. *Agricultural and Forest Meteorology*, 197, pp. 52–64. <https://doi.org/10.1016/j.agrformet.2014.06.007>
- Spinoni, J., Barbosa, P., De Jager, A., McCormick, N., Naumann, G., Vogt, J. V., Magni, D., Masante, D., and Mazzeschi, M., 2019. A new global database of meteorological drought events from 1951 to 2016. *Journal of Hydrology: Regional Studies*, 22(2019), pp. 1–24. <https://doi.org/10.1016/j.ejrh.2019.100593>
- Swain, S., Wardlow, B., Narumalani, S., Tadesse, T., and Callahan, K., 2011. Assessment of vegetation response to drought in nebraska using Terra-MODIS land surface temperature and normalized difference vegetation index. *GIScience and Remote Sensing*, 48(3), pp. 432–455. <https://doi.org/10.2747/1548-1603.48.3.432>
- Tarnavsky, E., and Bonifacio, R., 2020. Drought risk management using satellite-based rainfall estimates. In *Advances in Global Change Research*. Reading: Springer.
- Tsakiris, G., and Vangelis, H., 2004. Towards a Drought Watch System based on spatial SPI. *Water Resources Management*, 18(1), pp. 1–12. <https://doi.org/10.1023/B:WARM.000015410.47014.a4>
- UN-SPIDER 2020. Drought monitoring using the Standard Vegetation Index (SVI). En *Space-Based Information for Disaster Management and Emergency Response (UN-SPIDER)*. Último acceso: 13 de diciembre, 2020 de <https://un-spider.org/advisory-support/recommended-practices/recommended-practice-agricultural-drought-monitoring-svi>
- Wainwright, H. M., Steefel, C., Trutner, S. D., Henderson, A. N., Nikolopoulos, E. I., Wilmer, C. F., Chadwick, K. D., Falco, N., Schaettle, K. B., Brown, J. B., Steltzer, H., Williams, K. H., Hubbard, S. S., and Enquist, B. J., 2020. Satellite-derived foresummer drought sensitivity of plant productivity in Rocky Mountain headwater catchments: spatial heterogeneity and geological-geomorphological control. *Environmental Research Letters*, 15(8), pp. 1–10. <https://doi.org/10.1088/1748-9326/ab8fd0>
- Wang, D., Morton, D., Masek, J., Wu, A., Nagol, J., Xiong, X., Levy, R., Vermote, E., and Wolfe, R., 2012. Impact of sensor degradation on the MODIS NDVI time series. *Remote Sensing of Environment*, 119, pp. 55–61. <https://doi.org/10.1016/j.rse.2011.12.001>
- Xiangtao, W., Xianzhou, Z., Junhao, W., and Ben, N., 2020. Variations in the drought severity index in response to climate change on the Tibetan Plateau. *Journal of Resources and Ecology*, 11(3), pp. 304–314. <https://doi.org/10.5814/j.issn.1674-764x.2020.03.008>
- Zargar, A., Sadiq, R., Naser, B., and Khan, F. I., 2011. A review of drought indices. *Environmental Reviews*, 19(1), 333–349. <https://doi.org/10.1139/a11-013>